Journal of Marine Science and Technology

Volume 13 | Issue 2 Article 3

MOTION BEHAVIOR OF IMPACT OSCILLATOR

June-Yule Lee
Department of Electrical Engineering, Far East College, 49 Chung-Hua Road, Hsin-Shih Town, Tainan County, Taiwan 74404, juneyule@ms10.hinet.net

MOTION BEHAVIOR OF IMPACT OSCILLATOR

June-Yule Lee

Key words: impact oscillator, bifurcation diagram, poincare map, impact map.

ABSTRACT

This paper concerns a mass-spring-damper linear oscillator with endstop system. The parameter dependence of the impact oscillator is studied and the techniques of the bifurcation diagram, phase trajectory, impact map and Poincare map are applied. For the driving frequency ranges that no explicit solutions in analytical method, a complete bifurcation diagram is plotted using numerical solutions. Consequently, the phenomena of the complete, incomplete and chaotic chattering are classified as m-impact period-n motion using impact map and Poincare map.

INTRODUCTION

The impact oscillators arise whenever the components of a vibration system collide with rigid endstop or with each other. These oscillators widely occur in applications, such as the rattling gears [9], the vibrations of helicopter rotor blades [5], the fluctuation between the workpiece and cutting tool [4], the oscillations of the thermal expansion in pipe and tubes [7], the motion of a ship impacting against a harbor wall [14] and the motion of rigid blocks in an earthquake [8].

In references [1-3, 12-13, 15-16], researches were interested in the fundamentals of impact dynamics, particularly in the ensuing chaotic motion. Bifurcation theory was applied to investigate the stability of system behavior as parameter changed. Recently, the experimental signals of impacting system were investigated to confirm the previous results of the bifurcation diagram [10-11]. The recover ("clean") signals can be compared to the known phenomena to determine their origin. Thus, a better understanding of such an impact oscillators will benefit condition monitoring of a system. For this goal, a global and local dynamics need to be investigated.

In this paper, such an approach presented in [6] will be used to determine the stability of the impact oscillator. The parameter dependence of the impact oscillator will be illustrated using bifurcation diagram in terms of numerical solutions. In particular, a careful study of the effects on the dynamics of the oscillation by varying the forcing frequency and the restitution coefficient will be made. The numerical investigation of local dynamics, such as the complete, incomplete and chaotic chattering will also be characterized using impact map and Poincare map.

Paper Submitted 09/26/04, Accepted 12/27/04. Author for Correspondence: June-Yule Lee. E-mail: juneyule@ms10.hinet.net.

**Department of Electrical Engineering, Far East College, 49 Chung-Hua Road, Hsin-Shih Town, Tainan County, Taiwan 74404.*

IMPACT OSCILLATOR

The model considered here is a single degree of freedom system shown in Figure 1, where the mass is under a harmonic excitation and the motion is limited by an endstop. For simplicity, we assume the deformation during impact is negligible, the contact force resulting from impact is impulsive and the duration of the contact is much shorter than the period of the external excitation; in fact we idealize the impact as instantaneous. The equation of the motion when not impacting is

$$m\ddot{x} + 2c\dot{x} + kx = \cos\omega\tau, x > g \quad (1)$$

where $\ddot{x} = d^2x / d\tau^2$, $\dot{x} = dx / d\tau$, m is mass, c is damping ratio, k is spring, ω is driving frequency and g is the endstop. The impact occurs at $x(\tau) = g$ and the velocity change is modeled as $\dot{x}(\tau+) = -r\dot{x}(\tau-)$ where r is the restitution coefficient, $(\tau+)$ is the time after impact and $(\tau-)$ is the time before impact.

FLOW AND MAP

Equation (1) was defined in three dimensions space

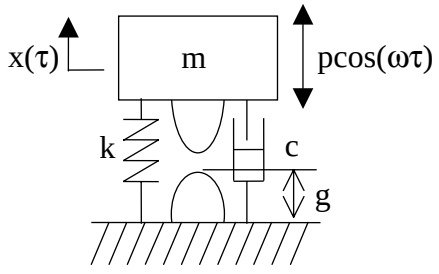

Fig. 1. Mass-spring-damper impact system.

as $(x, \dot{x}, \tau)$. The solutions flow in an infinite tube as τ evolves. We now define the phase φ by $\varphi = \tau \bmod T$ where $T = 2\pi/\omega$. This means we study the solution only every T seconds in τ. Thus the new phase space co9ordinate is $(x, \dot{x}, \varphi)$, where $0 \le \varphi \le T$. The solution projected onto the displacement and velocity plane is called phase trajectory. For periodic solutions, a closed trajectory will formed in the phase plane, see Figures 2(a) and 2(b). There are two different kinds of mapping in the $(x, \dot{x}, \varphi)$ space, which are Poincare return map and impact map.

1. Poincare map

Poincare return map gives two dimensions structure in plane instead of three dimensions flow in space, i.e. the solutions are projected onto a particular section $\varphi = \psi$ in $(x, \dot{x}, \varphi)$ space, where ψ is a constant in [0, T]. Thus Poincare map is a point set determined by its displacement and velocity $x(\tau)_{\varphi = \psi}$ in a section corresponding to a given constant phase $\varphi = \psi$. This definition is valid for all systems under periodic forcing function. A harmonic motion is a single point in return map, see Figure 2(d); a subharmonic motion of order n has a set of n points. In the case of the chaotic motion the map has a complex fractal structure.

2. Impact map

The impact map is related to the impact process. The point set in impact map is determined by impact velocity $\dot{x}(\tau_I)$ at $x(\tau_I) = g$ and impact phase $\varphi = \psi_I$, where

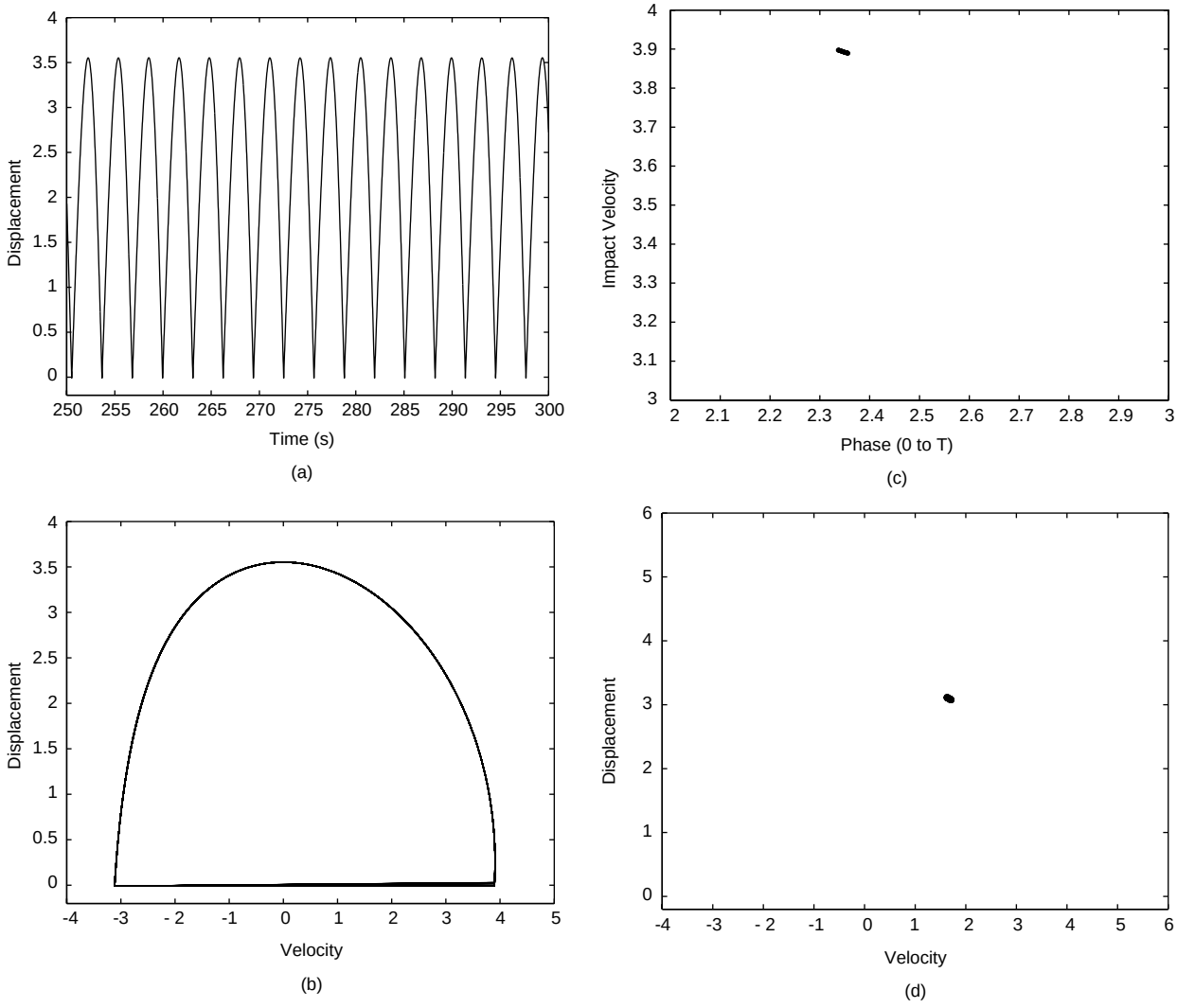

Fig. 2. Periodic chattering occurs at the driving frequency $\omega = 2$ with parameters $m = 1$, $c = 0.05$, $k = 1$, $r = 0.8$ and $g = 0$. (a) Displacement, (b) Phase trajectory, (c) Impact map shows 1-impact motion, and (d) Poincare map shows period-1 motion.

mod T and τ_I is the impact time. This definition is used to specify stability of impact dynamics. For a periodic impact motion, there is a single point in impact map, see figure 2(c), while m orders of subharmonic impact motion has m points. As the Poincare map, in the case of the chaotic motion the impact map has a complex fractal structure.

3. Discussion

Poincare map and impact map gave two dimensions structure in plane instead of three dimensions flow in space. Both maps are projected onto a particular section to enable identification the impact behavior. It is useful to describe the impact behavior using a pair of integers (m, n), where m is the number of the point set in impact map and n is the number of the return point set in Poincare map. This situation is referred to as a periodic m-impact period-n motion.

BIFURCATION DIAGRAM

In many applications one may be interested in global behavior depending on one of the parameters. The idea of the bifurcation diagram illustrates how the equilibrium state (point set in Poincare map or impact map) changes as a control parameter is gradually increased. In the following results, the point set in impact map is illustrated as the driving frequency changes.

1. Analytical solution

Using analytical methods, Shaw and Holmes [12], Shaw [13], Whiston [15-16] and Budd and Dux [1-3] have derived the following results.

2. Single-impact period-*n* motion

The periodic impact resonance occurs at the driving frequency $\omega = 2\omega_n$, where $\omega_n = \sqrt{k/m}$ is the fundamental frequency of the free mass oscillation. For example, in Figure 2 the fundamental impact resonance with single-impact period-1 impact motion occurs at the driving frequency $\omega = 2$.

3. Two-impact period-*n* motion

For some parameter combinations the impact motion may lose stability, i.e. the solution may bifurcate to high order impacts. The boundary of the control parameter where the systems lose their stability can be predicted using bifurcation theory. A boundary for period doubling was predicted in references [12-13], i.e. a stable single-impact period-n motion occurs in the region inside the boundary and two-impact period-n motion appears just outside the edge of the stable region.

4. Numerical solution

The following simulation results are obtained by numerical Runge-Kutta integration algorithm for Eq. (1). We fix the endstop at $g = 0$ and investigate the impact velocity in a periodic of time when the driving frequency changes. The data is displayed between 250 and 500 seconds, ignoring the first 250 seconds to make sure the system is in steady state.

In Figure 3, we show the bifurcation diagrams for various restitution coefficients r. For the case of $r = 0.6$ in Figure 3(d), the results agree with the analytical results show in references [1-3, 12-13, 15-16] where the impact resonance occur at $\omega = 2\omega_n$, $\omega_n = 1, 2, \ldots$ and so on. The peak amplitude of the impact velocity drops as ω increases. The motion transits from one-impact to two-impact at the driving frequency $\omega = 2.6$. As the driving frequency further increases the motion becomes unstable (chaotic) motion. For those ranges of the driving frequency that no explicit solutions in analytical method, a complete bifurcation diagram is plotted for full region of the driving frequency using numerical solutions.

In the case $r = 0$, see Figure 3(a), all of the mechanical energy is dissipated during the impacts, thus the mass essentially sticks to the endstop. There is no elastic rebound until the positive force drives the mass off again. This shows that the impact resonance at $\omega = 1$ is the fundamental resonance of the free oscillation. At $\omega_n = 2.6$, the period doubling bifurcation is clearly demonstrated. Figures 3(b)-3(f) demonstrate the results with coefficient $r = 0.2, 0.4, 0.6, 0.8$ and 0.9, respectively. The fundamental impact resonance is shifted form $\omega_n = 1$ to $\omega_n = 2$ as restitution coefficient increases.

CLASSIFICATION OF IMPACT MOTION

It is of practical interest to know where the stable and unstable boundaries are and what their structures are. Bifurcation diagrams in Figure 3 demonstrated three main parts of the boundary.

1. Complete chattering

As $\omega << 1$, the mass hits the endstop wall with a sufficiently low velocity, it resulted in a large number of impacts during the period of time $T = 2\pi/\omega$. For example, Figures 4(a) and (b) show the displacement and phase trajectory of the mass at $\omega = 0.2$. At time $t = 259$ seconds

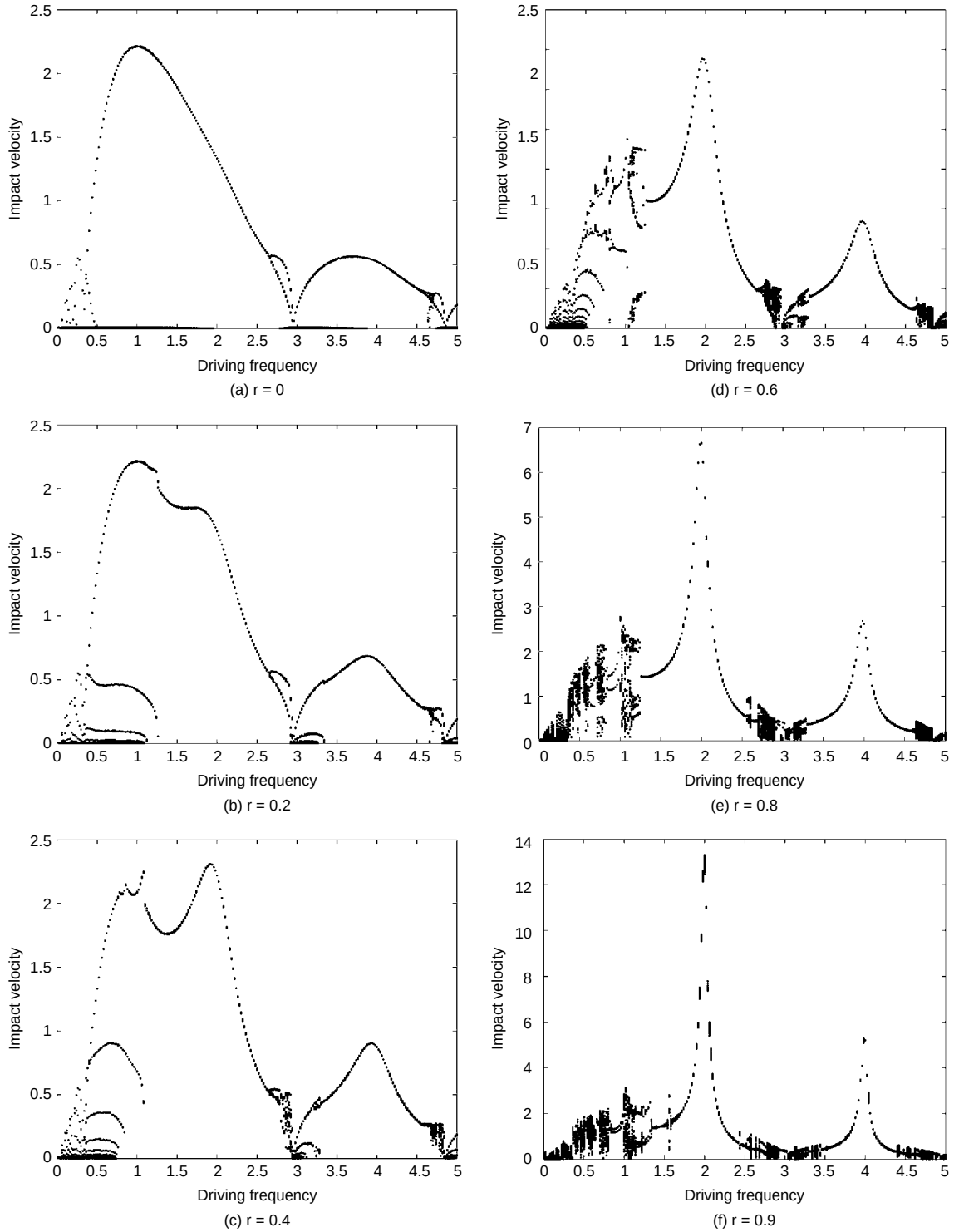

Fig. 3. Bifurcation diagrams for varying the driving frequency ω, where $m = 1$, $c = 0.05$, $k = 1$, $g = 0$ and (a) $r = 0$, (b) $r = 0.2$, (c) $r = 0.4$, (d) $r = 0.6$, (e) $r = 0.8$, and (f) $r = 0.9$.

the mass starts to hit the endstop and then rebounds back and forth until $t = 265$ seconds where the mass sticks to the wall. At $t = 275$ seconds the external driving force causes the mass to leave and then at $t = 290$ seconds the mass hit the endstop again. This is a case of periodic chattering, where $T = 31$ seconds. During the period of

time T, the mass eventually sticks to the endstop and cannot leave or enter until the next external positive force occurs. This process is described by a large number of points set in impact map, see Figure 4(c), and single point set in Poincare map, see Figure 4(d). We described this phenomenon as a complete chattering.

2. Incomplete chattering

When the driving frequency increases, the chattering oscillation does not stick to the endstop but leaves after a few numbers of impacts. This is because the external force provides a positive force to the mass sooner than the previous case. This process is classified as an incomplete chattering. Figures 5(a) and 5(b) show the displacement and the phase trajectory of the mass at driving frequency $\omega = 1.2$. This process is described by three clusters of point set in impact map and by two clusters of point set in Poincare map, see Figures 5(c) and 5(d).

3. Chaotic chattering

Figures 6(a) and 6(b) show the displacement and the phase trajectory of the mass at $\omega = 2.8$. The results demonstrate a complex structure. The "∞"-impact point set leads to a strange attractor in impact map, see Figure 6(c). In the same case plotted for Poincare map also demonstrated a period-"∞" fractal structure in Figure 6(d). Figures 7(a)-7(d) illustrate the Poincare maps for different phase sections, where φ are $\pi/4\omega$, $3\pi/4\omega$, $5\pi/4\pi$ and $7\pi/4\omega$, respectively. These results give us the information of how the flow is twisted in three dimensions space and also provide the evidences of the chaotic structure. We classify this characteristic as "∞"-impact period-"∞" motion.

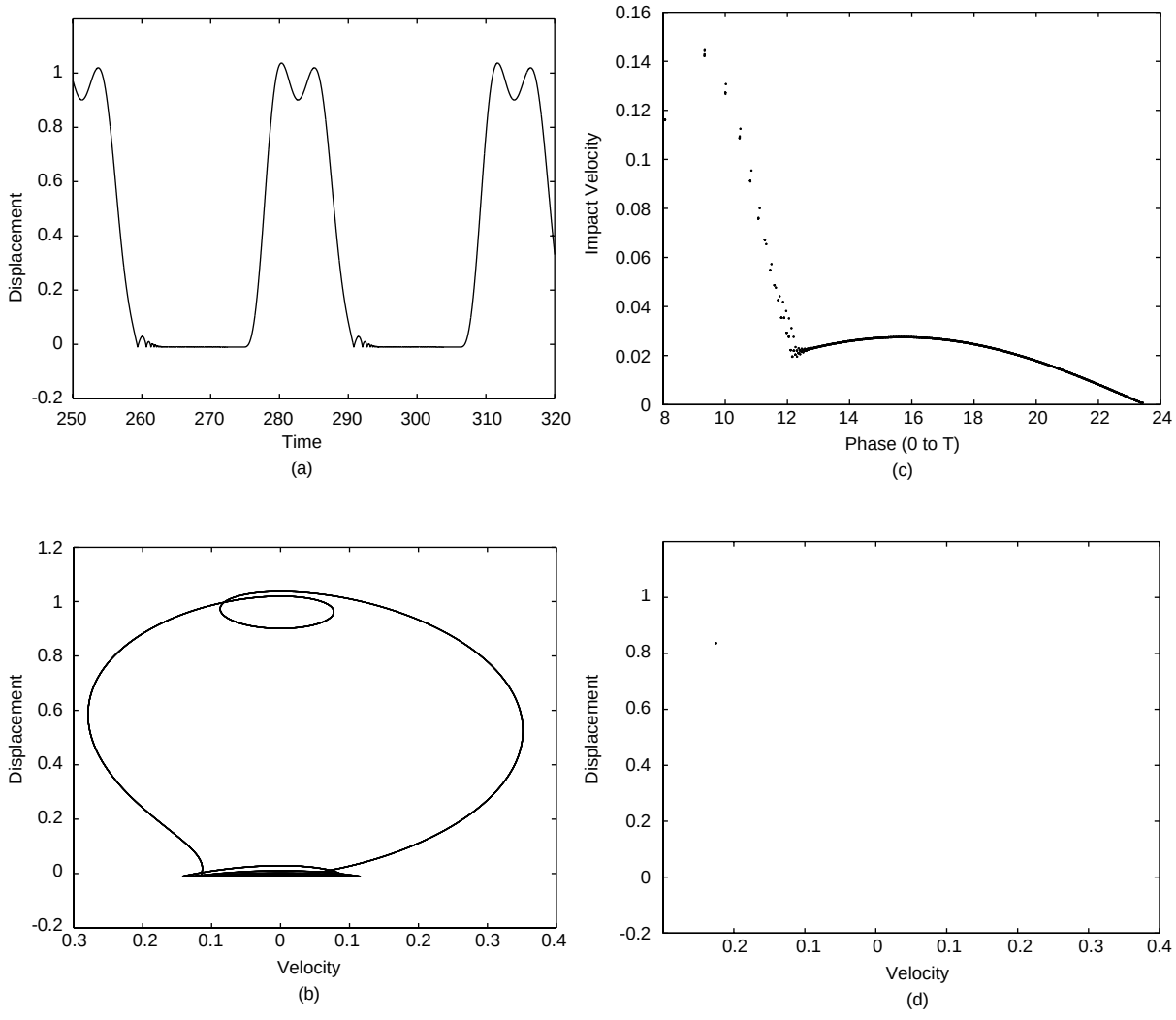

Fig. 4. Complete chattering occurs at the driving frequency $\omega = 0.2$ with parameters $m = 1$, $c = 0.05$, $k = 1$, $r = 0.8$ and $g = 0$. (a) Displacement, (b) Phase trajectory, (c) Impact map shows "∞ "-impact motion, and (d) Poincare map shows period-1 motion.

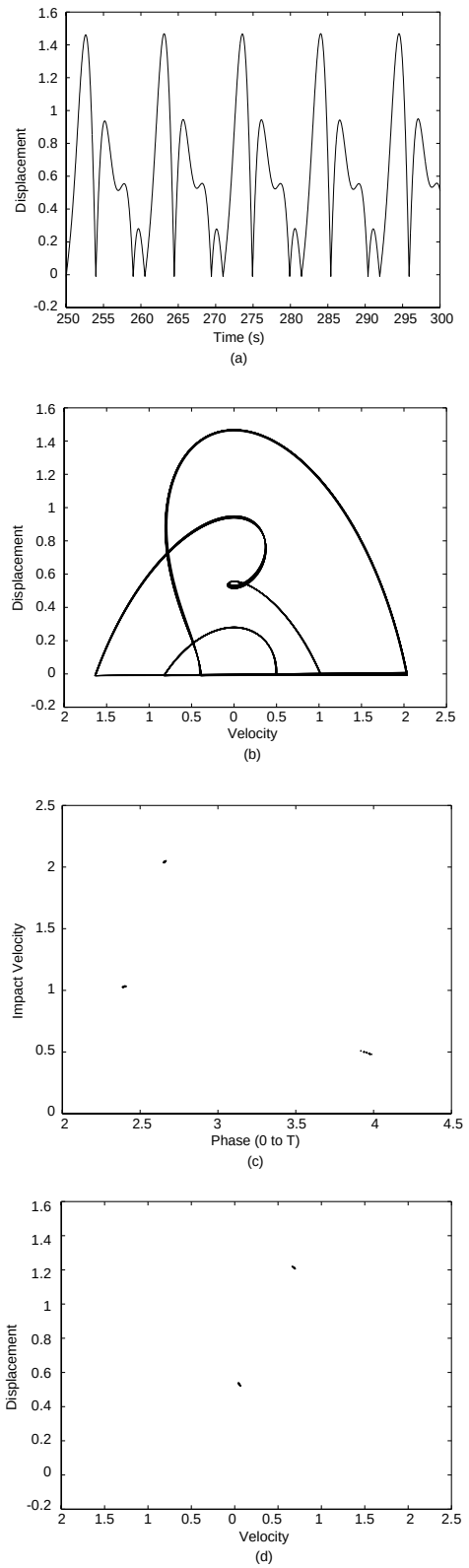

Fig. 5. Incomplete chattering occurs at the driving frequency ω = 1.2 with parameters m = 1, c = 0.05, k = 1, r = 0.8 and g = 0. (a) Displacement, (b) Phase trajectory, (c) Impact map shows 3-impact motion, and (d) Poincare map shows period-2 motion.

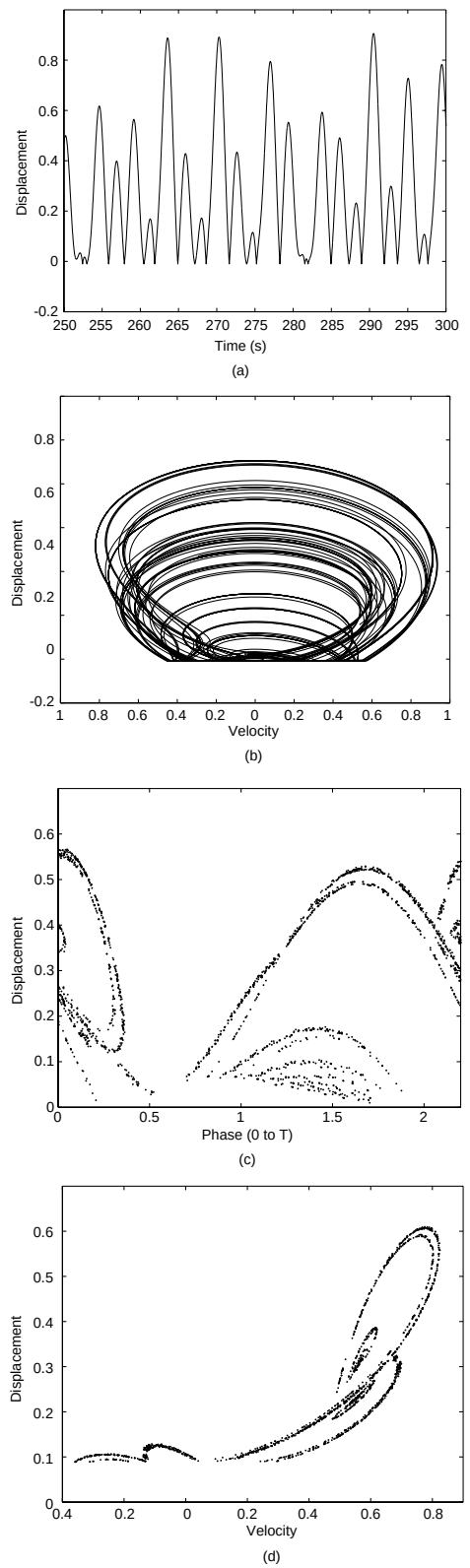

Fig. 6. Chaotic chattering occurs at the driving frequency ω = 2.8 with parameters m = 1, c = 0.05, k = 1, r = 0.8 and g = 0. (a) Displacement, (b) Phase trajectory, (c) Impact map shows "∞"-impact motion, and (d) Poincare map shows period-"∞" motion.

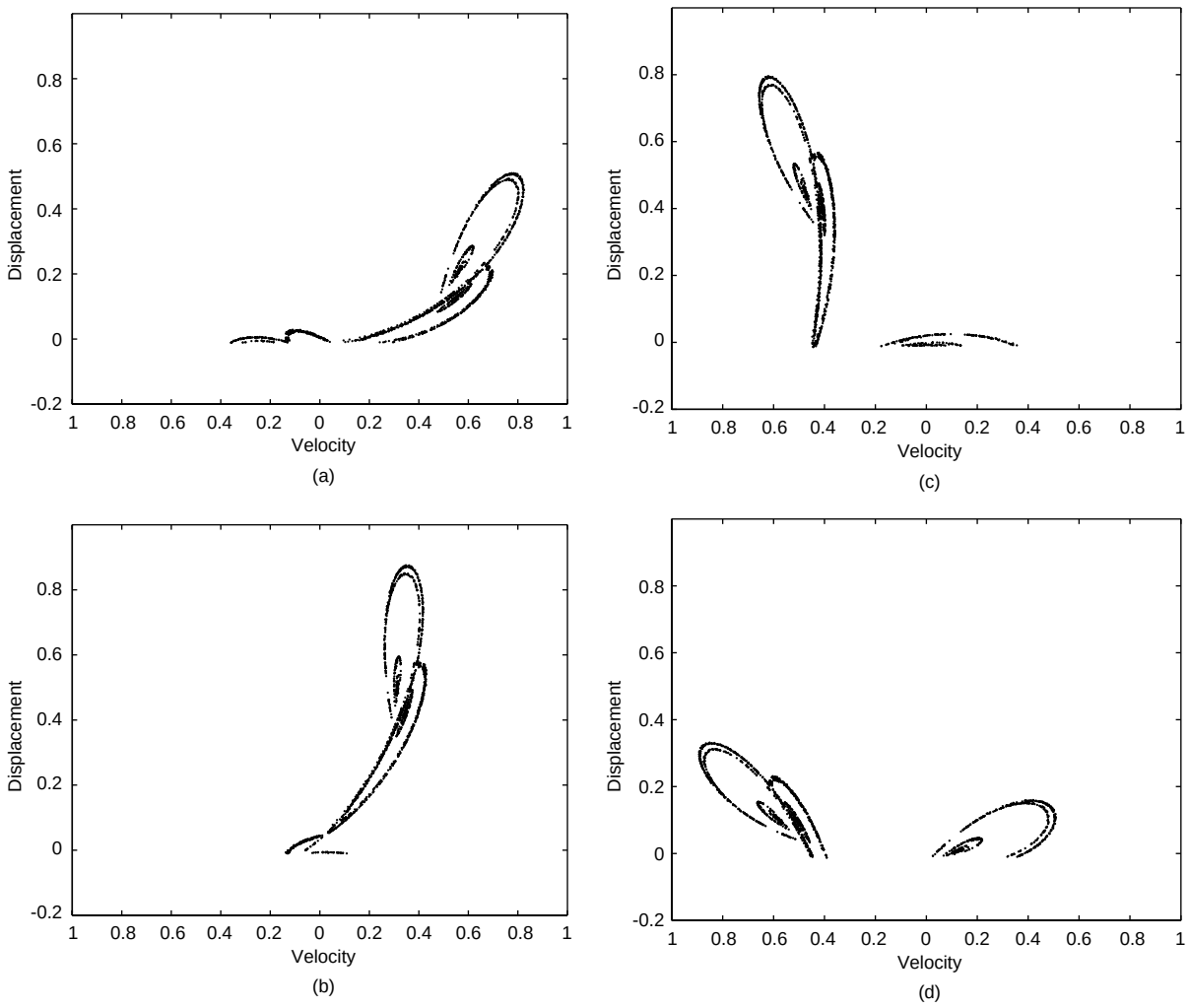

Fig. 7. Poincare maps at (a) $\varphi = \pi/4$, (b) $\varphi = 3\pi/4$, (c) $\varphi = 5\pi/4$, and (d) $\varphi = 7\pi/4$ for chaotic chattering in Figure 6.

CONCLUSION

The numerical solutions of a mass-spring-damper linear oscillator with endstop system were investigated. For the driving frequency ranges that no explicit solutions in analytical method, a complete bifurcation diagram was plotted in this paper. Consequently, the phenomena of the complete, incomplete and chaotic chattering were investigated using the impact map and Poincare map. These results provided a better understanding of such impacting systems and also benefited the condition monitoring of systems in terms of signal processing.

REFERENCES

1. Budd, C. and Dux, F., "Chattering and Related Behavior in Impact Oscillators," *Phil. Trans. R. Soc. London A*, Vol. 347, pp. 365-389 (1994).
2. Budd, C. and Dux, F., "Intermittency in Impact Oscillators Close to Resonance," *Nonlinearity*, Vol. 7, No. 4, pp. 1191-1224 (1994).
3. Budd, C. and Dux, F., "The Effect of Frequency and Clearance Variations on Single-Degree-of-Freedom Impact Oscillators," *J. Sound Vib.*, Vol. 184, No. 3, pp. 475-502 (1995).
4. Delio, T., Tlusty, J., and Smith, S., "Use of the Audio Signals for Chatter Detection and Control," *J. Eng. Ind. -T ASME*, Vol. 114, pp. 146-157 (1992).
5. Ehrich, F., "Some Observations of Chaotic Vibration Phenomena in High Speed Rotordynamics," *Proceedings of the 12th ASME Conference on Mechanical Vibration and Noise*, DE18-5, pp. 367-376 (1989).
6. Guckenheimer, J. and Holmes, P.J., *Nonlinear Oscillations, Dynamical Systems and Bifurcations of Vector Fields*, Springer-Verlag, New York (1993).

7. Goyder, H. and The, C., "A Study of the Impact Dynamics of Loosely Supported Heat Exchanger Tubes," *J. Press. Vess. Technol.*, Vol. 111, pp. 394-401 (1989).
8. Hogan, S.J., "On the Dynamics of Rigid Block Motion with Harmonic Forcing," *P. Roy. Soc. A–Math. Phy.*, Vol. 425, pp. 441-476 (1989).
9. Karagiannis, K. and Pfeiffer, F., "Theoretical and Experimental Investigation of Gear Rattling," *Nonlinear Dynam.*, Vol. 2, pp. 367-387 (1991).
10. Lee, J.-Y. and Nandi, A.K., "Blind Deconvolution of Impacting Signals Using High Order Statistics," *Mech. Syst. Signal Pr.*, Vol. 12, No. 2, pp. 357-371 (1998).
11. Lee, J.-Y. and Nandi, A.K., "Extraction of Impacting Signals Using Blind Deconvolution," *J. Sound Vib.*, Vol. 232, No. 5, pp. 945-962 (2000).
12. Shaw, S.W. and Holmes, P.J., "Periodically Forced Piecewise Linear Oscillator," *J. Sound Vib.*, Vol. 90, No. 1, pp. 129-155 (1983).
13. Shaw, S.W., "Forced Vibrations of a Beam with One-Sided Amplitude Constraint: Theory and Experiment," *J. Sound Vib.*, Vol. 99, No. 2, pp. 199-212 (1985).
14. Thompson, J.M.T., "Complex dynamics of Compliant Offshore Structures," *P. Roy. Soc. A–Math. Phy.*, Vol. 387, pp. 407-427 (1983).
15. Whiston, G.S., "Global Dynamics of a Vibro-Impacting Linear Oscillator," *J. Sound Vib.*, Vol. 118, No. 3, pp. 395-429 (1987).
16. Whiston, G.S., "Singularities in Vibro-Impact Dynamics," *J. Sound Vib.*, Vol. 152, No. 3, pp. 427-460 (1992).